• Basic Research •

Molecular mechanism of hypoxia and alpha-ketoglutaric acid on collagen expression in scleral fibroblasts

Yun Sun, Zhuo-Zheng Li, Jing Yang, Ya-Ru Sha, Xin-Yu Hou, Hong Fu, Jia-Yin Li, Shu-Chang Bai, Yong-Fang Xie, Guo-Hui Wang

School of Life Science and Technology, Shandong Second Medical University, Weifang 261053, Shandong Province, China

Correspondence to: Guo-Hui Wang and Yong-Fang Xie. School of Life Science and Technology, Shandong Second Medical University, Weifang 261053, Shandong Province, China. wangguohui1983@163.com; xieyongfang@sdsmu.edu.cn

Received: 2024-03-10 Accepted: 2024-07-23

Abstract

● **AIM:** To investigate the molecular mechanisms underlying the influence of hypoxia and alpha-ketoglutaric acid (α-KG) on scleral collagen expression.

● **METHODS:** Meta-analysis and clinical statistics were used to prove the changes in choroidal thickness (ChT) during myopia. The establishment of a hypoxic myopia model (HYP) for rabbit scleral fibroblasts through hypoxic culture and the effects of hypoxia and α-KG on collagen expression were demonstrated by Sirius red staining. Transcriptome analysis was used to verify the genes and pathways that hypoxia and α-KG affect collagen expression. Finally, real-time quantitative reverse transcription polymerase chain reaction (RT-qPCR) was used for reverse verification.

● **RESULTS:** Meta-analysis results aligned with clinical statistics, revealing a thinning of ChT, leading to scleral hypoxia. Sirius red staining indicated lower collagen expression in the HYP group and higher collagen expression in the HYP+α-KG group, showed that hypoxia reduced collagen expression in scleral fibroblasts, while α-KG can elevated collagen expression under HYP conditions. Transcriptome analysis unveiled the related genes and signaling pathways of hypoxia and α-KG affect scleral collagen expression and the results were verified by RT-qPCR.

● **CONCLUSION:** The potential molecular mechanisms through which hypoxia and α-KG influencing myopia is unraveled and three novel genes *TLCD4*, *TBC1D4*, and *EPHX3* are identified. These findings provide a new perspective on the prevention and treatment of myopia *via* regulating collagen expression.

● **KEYWORDS:** sclera; scleral collagen expression; hypoxia; alpha-ketoglutaric acid; myopia

DOI:10.18240/ijo.2024.10.03

Citation: Sun Y, Li ZZ, Yang J, Sha YR, Hou XY, Fu H, Li JY, Bai SC, Xie YF, Wang GH. Molecular mechanism of hypoxia and alpha-ketoglutaric acid on collagen expression in scleral fibroblasts. *Int J Ophthalmol* 2024;17(10):1780-1790

INTRODUCTION

Myopia, commonly known as short-sightedness or nearsightedness, is a prevalent condition typically onset during childhood. The causative factors for myopia encompass both genetic and environmental elements[1]. Projections indicate that nearly 50% of the global population will be myopic by 2050, with uncorrected refractive errors identified as a primary cause of visual impairment[2-3]. Consequently, myopia prevention emerges as the optimal strategy to mitigate pathological myopia and its associated complications[4]. Despite its prevalence, the mechanisms underlying myopia remain elusive, underscoring the imperative need to identify causative factors and develop effective strategies for prevention and treatment.

The sclera, serving as the principal connective tissue of the eyes, plays a pivotal role in vision[5]. Scleral remodeling impacts the onset and progression of myopia[6]. Furthermore, collagen metabolism influences scleral mechanical properties and remodeling[7]. The choroid functions as the ocular vascular layer, delivering oxygen and nutrients to the retina and sclera. In myopia patients, choroidal blood perfusion is diminished[8-9], leading to scleral ischemia and hypoxia. Recent studies have shown that myopia and scleral remodeling are related to hypoxia, resulting in the activation of the hypoxia-inducible factor-1α (HIF-1α) signaling pathway and reduced collagen expression in human scleral fibroblasts[10]. Hypoxia-induced up-regulation of HIF-2α further contributes to the degradation of collagen type I α1 by elevating matrix metallopeptidase 2 (MMP-2) expression[11]. HIF-1 regulates collagen prolyl-4-hydroxylase 1 (P4HA1) and P4HA2 expression in fibroblasts, promoting collagen deposition[12]. Hypoxia also stimulates

collagen synthesis in keloid fibroblasts[13]. Therefore, the effect of hypoxia on collagen expression in different cells is inconsistent.

Alpha-ketoglutaric acid (α-KG), a crucial intermediate metabolite in the tricarboxylic acid cycle, is involved in the hypoxia signaling pathway and collagen biosynthesis. α-KG has been shown to enhance collagen hydroxylation by increasing P4HA activity in breast cancer cells, consequently elevating collagen expression[14]. In lung myofibroblasts, α-KG may promote collagen expression by activating mTOR complex 1[15]. Notably, collagen hydroxylase P4HA1 in breast cancer cells enhances HIF-1 protein stability by reducing α-KG availability and generating succinate[16]. Consequently, we posit that α-KG plays a role in collagen synthesis and the regulation of the HIF-1α signaling pathway, thereby influencing scleral remodeling.

In this experiment, we successfully extracted and cultured rabbit scleral fibroblasts, establishing a hypoxic myopia cell model (HYP). Sirius red staining was employed to investigate the impact of hypoxia and α-KG on scleral fibroblast collagen. Transcriptome sequencing elucidated the effects of hypoxia and α-KG on the transcriptional profile of scleral fibroblasts, with subsequent gene ontology (GO) and Kyoto Encyclopedia of Genes and Genomes (KEGG) functional enrichment analyses shedding light on the molecular mechanisms influencing collagen expression. Validation of newly identified genes was achieved through real-time quantitative reverse transcription polymerase chain reaction (RT-qPCR), presenting innovative insights and theoretical guidance for comprehending myopia-related molecular mechanisms and advancing the prevention and treatment of myopia.

MATERIALS AND METHODS

Ethical Approval The study was approved by the Ethics Committee of the Shandong Second Medical University (No.2023SDL129). The study was conducted in accordance with the principles of the Declaration of Helsinki. The informed consent was obtained from the subjects. The study was conducted in accordance with the ARVO Statement for the Use of Animals in Ophthalmic and Vision Research.

Changes in Choroidal Thickness in Myopia

Meta-analysis Theme words “myopia” and “thickness” were used for literature searches on PubMed. Review Manager 5.4 was employed for Meta-analysis, excluding documents with inconsistent parameters.

Clinical study of choroidal thickness in myopia children Choroidal thickness (ChT) tests were conducted on children aged 6–12y at the Ophthalmic Center of the Affiliated Hospital of Shandong Second Medical University. All cases in this study were mild or moderate myopia (-0.50 D ≥ equivalent spherical lens>-6.00 D after cycloplegia; The curvature is between 42.0 and 42.0 D, and the vision can be corrected to 0). There were 11 males (22 eyes) and 14 females (28 eyes) aged 8.13±1.8 years old, and there was no significant difference in general clinical data between the two groups. All myopic children underwent post-cycloplegic optometry, eye axe, and ChT (averaging 3 measurements) using Spectralis-enhanced depth imaging optical coherence tomography mode at initial examination and re-examination after 6mo. To minimize operational errors, all inspections were carried out by the same inspector. To avoid the influence of diurnal variation on ChT results, all subjects were examined between 14:00 and 16:00, and in the undilated state to avoid interference with data caused by anticholinergic drugs such as tropicamide.

Extraction and Treatment of Rabbit Scleral Fibroblasts

Extraction of scleral fibroblasts Scleral tissue extracted from 1-month-old New Zealand white rabbits, cut into small pieces no more than 1 mm^3. Collagenase II was added for tissue breakdown; cells were cultured in Dulbecco’s modified Eagle’s medium/F12 medium with 2× penicillin-streptomycin and 15% fetal bovine serum at 37°C, 5% CO_2. In about 1wk, a single cell can be seen sticking to the wall, or cells can climb out of the edge of the tissue.

Treatment of scleral fibroblasts After adhesion, cells were treated with 5% O_2 for a hypoxia model or medium containing 2 mmol/L α-KG for 24h.

Collagen Expression Determined by Sirius Red Sirius red staining method used to detect intracellular collagen expression in this experiment was referred to the relevant references[17], and Image J was utilized for semi-quantitative analysis.

Transcriptome Sequencing

Total RNA extraction and quality control Trizol was employed for RNA extraction. RNA sample concentration ≥100 ng/μL, total amount >2 μg, OD260/280 value between 1.8 and 2.2, OD260/230 ≥2.0, and RIN detected by Agilent 2100 Bioanalyzer ≥6.5.

Preparation and quality control of total RNA-seq library Magnetic beads with oligo-dT were used for to enrichment and purification of mRNA. The elution-bound mRNA was thermally fractured so that the fragments were distributed between 100–300 bp. Synthesize the first cDNA, hydrolyze and digest the RNA, synthesize the two-strand cDNA and the double-strand cDNA was purified by Agencourt AMpure XP magnetic beads. Add the end complement system, at the same time, a single adenylate “A” is added to the end-modified double-stranded cDNA 3’ ends to prevent flat-end self-linking. T4 DNA ligase was used to connect illumina sequencing splices to both ends of the library DNA, used an Agencourt SPRI select nucleic acid fragment screening kit to screen fragment size. The cDNA library was amplified by PCR, and the library concentration and fragment length distribution were detected by Qubit and Agilent 2100 Bioanalyzer. The

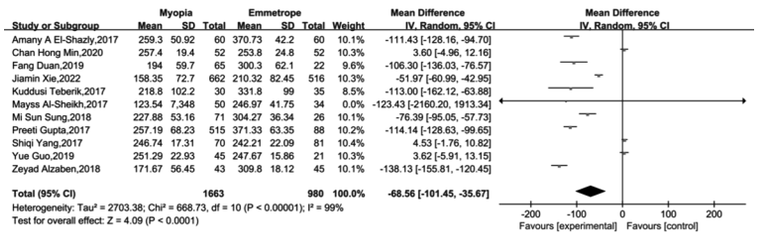

Figure 1 Forest map illustrating the Meta-analysis results of choroidal thickness in myopic and emmetropic individuals SD: Standard deviation; Total: Sample size.

required concentration was >5 ng/μL, and the fragment length was concentrated between 300–400 bp. The library was finally sequenced in illumina high-throughput sequencing platform with 2×150 bp double-ended sequencing mode.

RNA-seq data processing methods 1) Raw data filtering with FastQC and R packages for obtaining high-quality clean data. 2) STAR software for read alignment, Picard for data analysis, such as calculating the distribution and base proportion of different samples in introns, exons, and gene spacer regions, and was also used to analyze the saturation and redundant sequences of samples. 3) RSeQC software was used to randomly extract and compare sequences contained in the reference genome, and the extracted fragments were used for expression quantitation and mRNA analysis of the transcript. 4) The expression level (FPKM value) of each obtained RNA was counted, and StringTie was used to quantify the expression of the transcript and compare the FPKM value of samples from different groups. Deseq2 software was used to analyze the differentially expressed genes. The differential genes need to satisfy P<0.05 and |log2 (fold change)| >1, where log2 (fold change) >1 was labeled as up-regulated (Up), log2 (fold change) <-1 was labeled as down-regulated (Down), and the marker that does not meet the above conditions is non-significant differentially expressed genes (Not DEG). Use Morpheus to draw the heat map. 5) Using cluster Profiler for GO analysis and KEGG analysis. According to the P, the most significantly enriched 10 GO items in the biological processes (BP), cell components (CC), and molecular functions (MF) categories were screened respectively. KEGG enrichment analysis annotated the differentially expressed genes into databases such as metabolic pathway databases and calculated the normalized enrichment scores through hypergeometric tests to determine the proportion of differentially expressed genes in a GO or metabolic pathway. The significantly up or down-regulated genes were located at the top or bottom of the gene set. The thresholds for the above analysis are P<0.05 and adjust P<0.05.

RT-qPCR RNA was reverse transcribed to cDNA using a PCR reverse transcription kit. Amplification was performed on a PCR apparatus (Roche 810), and the final cDNA obtained was stored at -30°C. cDNA was used as a template for qPCR and performed on a PCR apparatus with SYBR Green PCR Master Mix. The primer sequences used were listed in Table 1. Relative mRNA expression was calculated using the $2^{-\Delta\Delta Ct}$ method.

Table 1 Primers for intersecting genes

Gene information	Forward primer sequence	Reverse primer sequence
β-actin	CCAGCTGCCGACCACC	ATCCATGGTGAGCTGAGCG
TLCD4	TACGCATTGCCACGATACCAC	TGCTCCAAGTCTTTCGTAGGGT
TBC1D4	CAGCCCAGTGTATGCTACCG	TCATGCGGCTGCCAAATACC
EPHX3	GGCTCACAGGACCCATCAAC	CAGCCCCAGCTCGAAGTAAG

Statistical Analysis Statistical analysis was performed using GraphPad Prism 8 software. Continuous variables were represented by mean±standard deviation (mean±SD), and a paired t-test was used for comparison between the two groups. The test level was α=0.05.

RESULTS

Choroidal Thickness Meta-Analysis Results The Meta-analysis findings underscored a significant reduction in ChT among individuals with myopia. The choroid, replete with capillaries supplying oxygen and nutrients to the sclera and retina, plays a pivotal role in modulating choroidal blood perfusion. In an effort to elucidate the impact of myopia on the human choroid, a comprehensive search of PubMed spanning the years 2017 to 2022 yielded 462 pertinent literature articles. Following a meticulous review of titles and content, 358 articles were excluded due to their lack of relevance to the research. Subsequently, a thorough examination of the remaining 104 articles identified 11 sources containing the requisite data. The amalgamated data encompassed 1663 myopic patients and 980 normal controls. Meta-analysis of the compiled data was performed, with the results depicted in Figure 1. The forest plot illustrates that ChT in individuals with myopia was notably thinner compared to emmetropic individuals[18-28]. The results showed that ChT was thinner in patients with myopia.

Choroidal Thinning During Myopia Progression in Children Biological parameters of myopic children's eyes attending the optometry clinic or undergoing physical examinations at the Ophthalmic Center of the Affiliated Hospital of Shandong Second Medical University between November 2021 and June 2022 were detailed in Table 2. The spherical equivalent of myopic children measured

Table 2 Comparison of ocular biological parameters in the first measurement and after 6mo mean±SD

Parameters	Total eye count	Before[a]	6mo	*P*
SE, D	50	-2.71±1.15	-3.46±1.15	<0.01
AL, mm	50	23.92±0.72	24.35±0.77	<0.01
ChT, μm	50	302.21±10.37	296.14±10.45	<0.01

SE: Spherical equivalent; AL: Axial length; ChT: Choroidal thickness. [a]The first measurement.

-2.71±1.15 D initially and -3.46±1.15 D after 6mo. The axial length measured 23.92±0.72 mm at the first assessment and increased to 24.35±0.77 mm after 6mo. Notably, over the 6mo period, the eye axis of the 25 children lengthened, and eye refraction increased, indicative of ongoing myopia development.

ChT levels measured twice before and after 6mo were 302.21±10.37 and 296.14±10.45 μm, respectively, indicating a significant thinning of ChT. Clinical statistical results consistently mirrored the findings of the Meta-analysis, demonstrating that myopia progression coincided with axial lengthening, increased refraction, and decreased ChT. These changes, in turn, influenced choroidal blood perfusion, leading to choroidal-scleral hypoxia. The observed correlation suggests that hypoxia may be a contributing factor to induced myopia and scleral remodeling.

Impact of Hypoxia and α-KG on Collagen Expression in Scleral Fibroblasts To discern the effects of hypoxia and α-KG on collagen expression, rabbit scleral fibroblasts were extracted and cultured. Subsequent to extraction, cells underwent treatment with hypoxia (5% O_2) in a three-gas incubator or were exposed to a culture medium enriched with 2 mmol/L α-KG. Collagen expression was visualized through Sirius red staining (Figure 2). Notably, collagen expression in scleral fibroblasts within the HYP group was substantially lower than that in the control group. Conversely, the introduction of α-KG markedly elevated collagen expression in scleral fibroblasts under hypoxia conditions. These findings unequivocally demonstrate the significant influence of both hypoxia and α-KG on collagen expression in rabbit scleral fibroblasts.

RNA-seq Analysis of Scleral Fibroblasts under Hypoxia and α-KG Treatment

Differential gene expression analysis Scleral fibroblasts underwent treatment with hypoxia and α-KG, followed by sample collection, total RNA extraction, and quality control for sequencing analysis. In the RNA-seq data analysis, principal component analysis (PCA) was employed to reduce the dimensionality of the entire genome information dataset. PCA utilizes the most crucial features to represent all expression information, ensuring the selected new feature variables are uncorrelated. As depicted in Figure 3, the linear distance between the control group, HYP group, and HYP+α-KG group was substantial, indicating significant differences between the groups. This suggests that hypoxia and α-KG exert a pronounced effect on the gene expression profile of scleral fibroblasts.

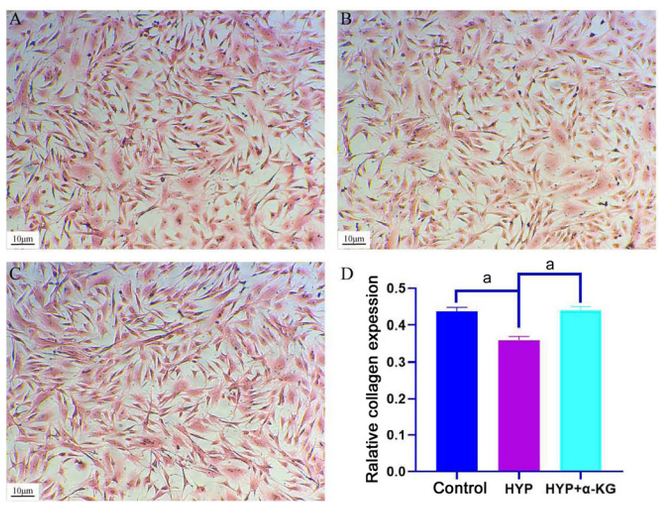

Figure 2 Sirius red staining results for sclera fibroblasts A: Control group; B: HYP group; C: HYP+α-KG group; D: Relative collagen content in control, HYP, and HYP+α-KG groups; [a]*P*<0.001; Scale: 10 μm. HYP: Hypoxic myopia model; KG: Ketoglutaric acid.

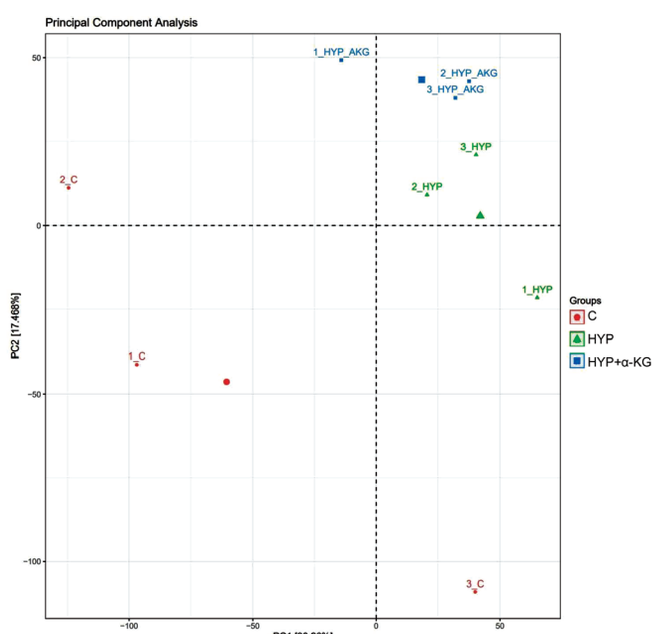

Figure 3 PCA analysis results of different treatment groups The red dot represents the three replicates of the control group, the green triangle represents the three replicates of the HYP group, and the blue square represents the three replicates of the HYP+α-KG group. PCA: Principal component analysis; C: Control; HYP: Hypoxic myopia model; KG: Ketoglutaric acid.

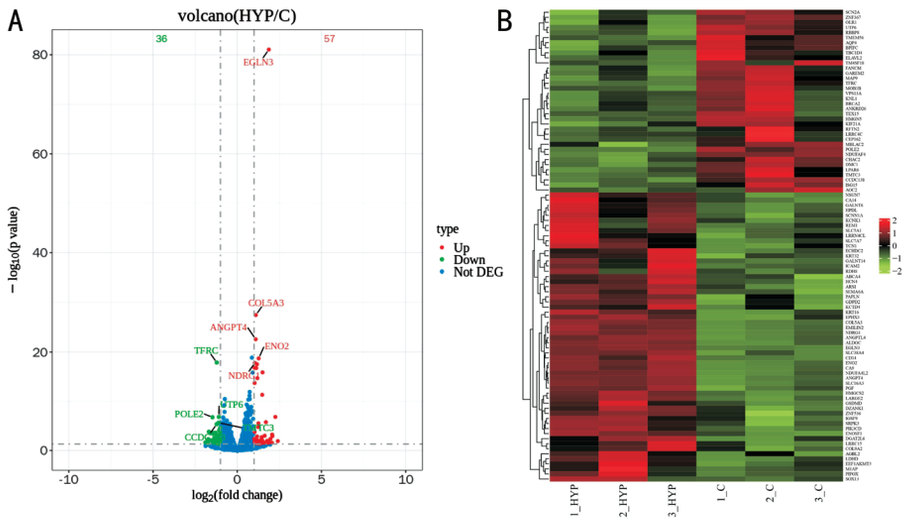

Figure 4 Volcano map (A) and cluster analysis map (B) of differentially expressed genes of HYP *vs* control A: Red dots signify Up genes, green dots denote Down genes, and blue dots represent Not DEG. The ordinate of the volcano map represents the value of -lg*P*, with smaller *P* values indicating greater significance of differences. B: It portrays high repeatability across samples, where each column represents a different group, and each row represents a distinct gene. Up: Up-regulated; Down: Down-regulated; Not DEG: Non-significant differentially expressed genes; C: Control; HYP: Hypoxic myopia model.

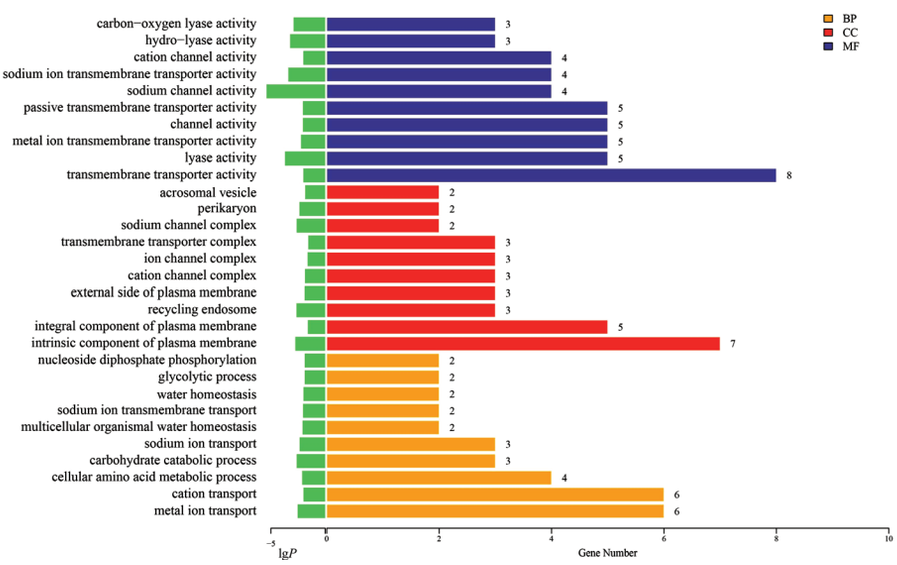

Figure 5 Gene ontology classification statistics of HYP *vs* control differentially expressed genes (top 10) BP: Biological processes; CC: Cell components; MF: Molecular functions; HYP: Hypoxic myopia model.

RNA-seq Unveils the Impact of Hypoxia on Collagen Expression in Scleral Fibroblasts

Differential gene screening Differential expression analysis using Deseq2 software for HYP *vs* control revealed 91 differentially expressed genes, with 56 Up and 35 Down genes (Figure 4).

Enrichment analysis of differential genes The top 10 GO functions significantly enriched in BP, CC, and MF were illustrated in Figure 5. The results highlighted MF related to hypoxia, including the activity of carbon-oxygen lyase. CC encompassed cellular components associated with ion channels, with BP reflecting alterations in the cellular glycolysis process, potentially linked to energy production reduction by hypoxia and subsequent inhibition of extracellular matrix production and collagen synthesis.

The Figure 6 scatterplot showcases the enrichment of KEGG pathways, with the HIF-1 signaling pathway and the peroxisome proliferators-activated receptors (PPAR) signaling pathway prominently enriched among HYP *vs* control differentially expressed genes. Notably, the HIF-1 signaling pathway exhibited significant enrichment, as indicated by the upper-right positioning of the dot representing this pathway.

These analyses shed light on the intricate molecular responses of scleral fibroblasts to hypoxia, emphasizing the modulation of collagen expression and key signaling pathways.

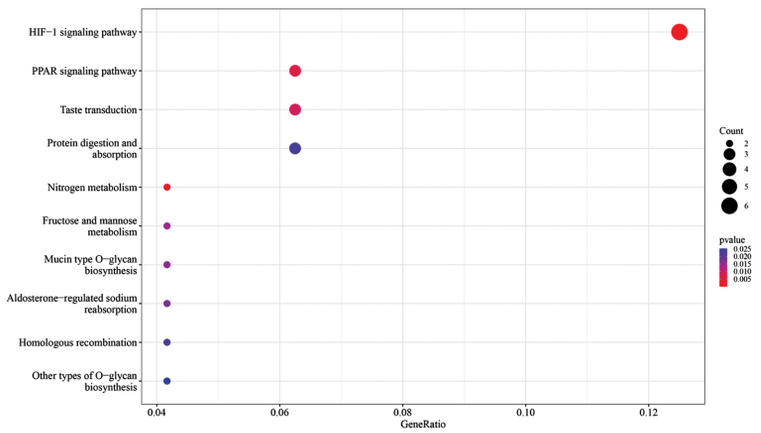

Figure 6 Scatterplot of KEGG pathway enrichment analysis for HYP *vs* control differentially expressed genes KEGG: Kyoto Encyclopedia of Genes and Genomes; HIF: Hypoxia-inducible factor; PPAR: peroxisome proliferators-activated receptors; HYP: Hypoxic myopia model.

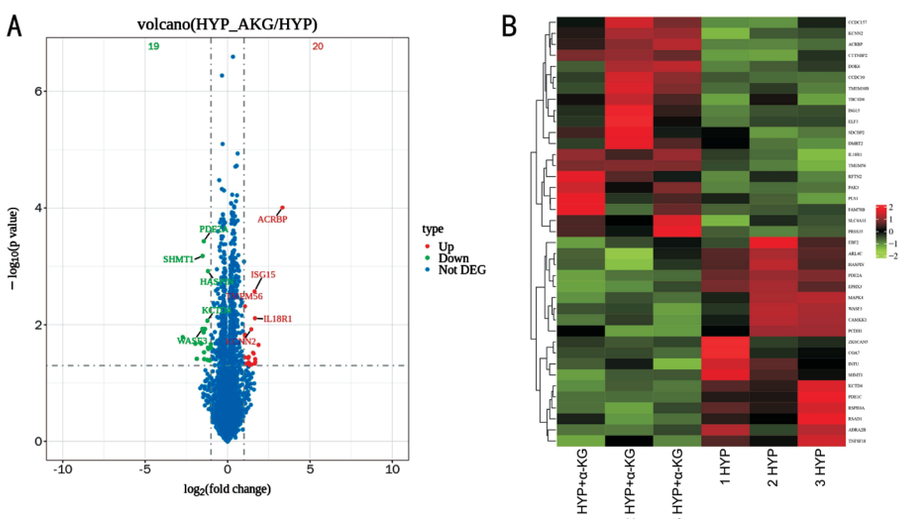

Figure 7 Volcano map (A) and cluster analysis map (B) of differentially expressed genes of HYP+α-KG *vs* HYP A: Red dots denote Up genes, green dots represent Down genes, and blue dots indicate Not DEG; B: Emphasizes the notable alterations in gene expression patterns. Up: Up-regulated; Down: Down-regulated; Not DEG: Non-significant differentially expressed genes; HYP: Hypoxic myopia model; KG: Ketoglutaric acid.

RNA-seq Unveils the Impact of α-KG on Collagen Expression in Scleral Fibroblasts

Differential gene screening Differential expression analysis for HYP+α-KG *vs* HYP revealed 37 differentially expressed genes, comprising 20 Up and 17 Down genes (Figure 7).

Enrichment analysis of differential genes The top 10 GO functions are depicted in Figure 8. Notably, MF related to actin binding and cytoskeletal protein binding, along with CC and BP associated with cytoskeleton-related components and processes, were significantly altered. These findings suggest that α-KG treatment activated diverse biological processes in scleral fibroblasts in response to HYP stimulation, potentially inhibiting hypoxia-related biological changes.

The Figure 9 scatterplot reveals the enrichment of KEGG pathways, with the Morphine addiction signaling pathway prominently enriched among HYP+α-KG *vs* HYP differentially expressed genes. Given Morphine's association with collagen expression, the result suggests that α-KG might enhance collagen expression through a signaling pathway, thereby potentially contributing to improved eye growth and development.

RT-qPCR Verification of New Genes Discovered by RNA-seq The Venn diagram in Figure 10 illustrates the intersection of differentially expressed genes between HYP *vs* control and HYP+α-KG *vs* HYP. Three genes, namely *ISG15*, *TLCD4*, and *TBC1D4*, were identified at the intersection of decreased expression in HYP *vs* control and increased expression in HYP+α-KG *vs* HYP. Additionally, one gene, *EPHX3*, was identified at the intersection of increased expression in HYP *vs* control and decreased expression in HYP+α-KG *vs* HYP.

Studies have reported the relationship between *ISG15* and collagen. RT-qPCR verification was conducted on the intersection genes *TLCD4*, *TBC1D4*, and *EPHX3*.

The results, depicted in Figure 11, demonstrated the consistency of the RT-qPCR results with the trends observed in RNA-seq, providing robust confirmation of the expression changes in the identified intersection genes.

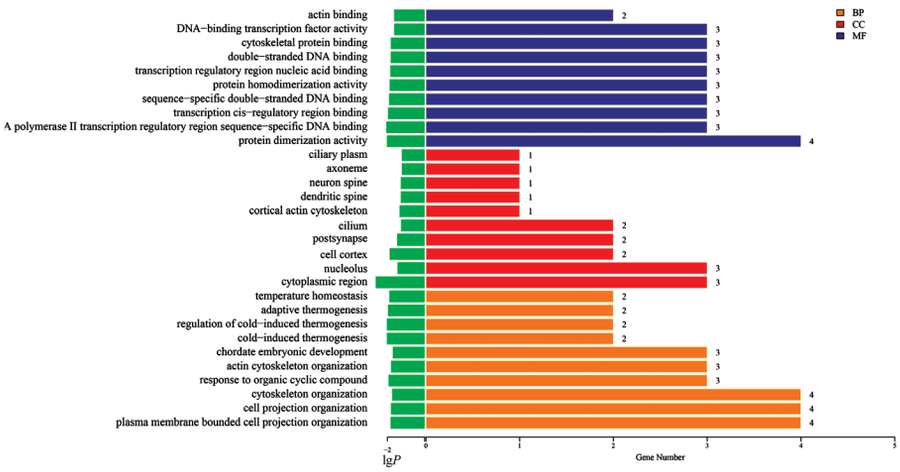

Figure 8 Gene ontology classification statistics of HYP+α-KG *vs* HYP differentially expressed genes (top 10) BP: Biological processes; CC: Cell components; MF: Molecular functions; HYP: Hypoxic myopia model; KG: Ketoglutaric acid.

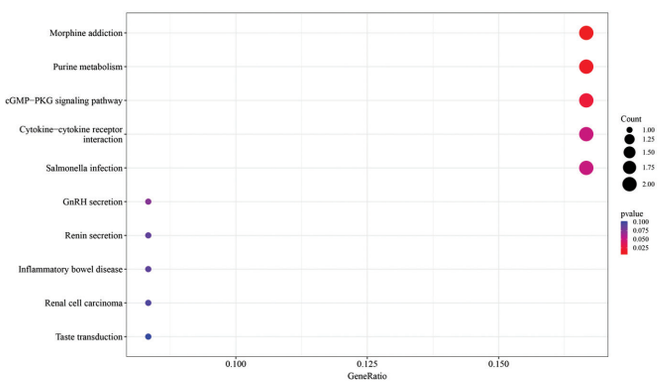

Figure 9 Scatterplot of KEGG pathway enrichment analysis of HYP+α-KG *vs* HYP differentially expressed genes KEGG: Kyoto Encyclopedia of Genes and Genomes; HYP: Hypoxic myopia model; KG: Ketoglutaric acid.

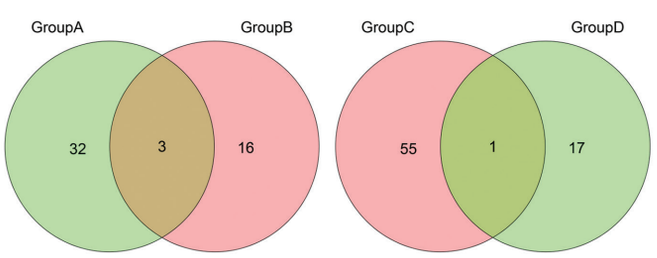

Figure 10 Venn diagram of differentially expressed genes Group A: HYP *vs* control Down genes; Group B: HYP+α-KG *vs* HYP Up genes; Group C: HYP *vs* control Up genes; Group D: HYP+α-KG *vs* HYP Down genes. Up: Up-regulated; Down: Down-regulated; HYP: Hypoxic myopia model; KG: Ketoglutaric acid.

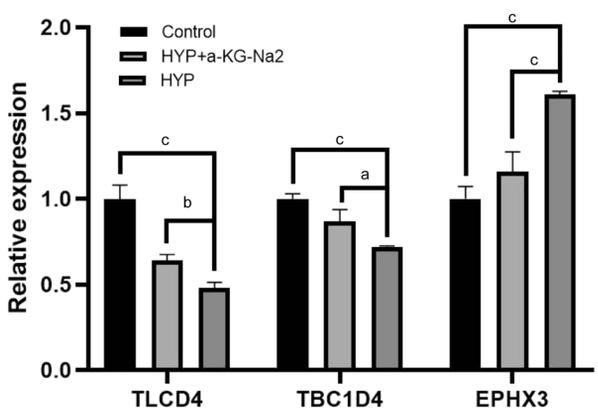

Figure 11 RT-qPCR results for the intersection genes of HYP *vs* control and HYP+α-KG *vs* HYP [a]*P*<0.05; [b]*P*<0.01; [c]*P*<0.001. HYP: Hypoxic myopia model; KG: Ketoglutaric acid; RT-qPCR: Real-time quantitative reverse transcription polymerase chain reaction.

DISCUSSION

The refractive state of the eye can be divided into orthotropia and ametropia. Myopia is a type of ametropia in the eye. That is, the external parallel light passing through the refractive system of the eye focuses on the refractive state in front of the macular fovea. Since the outbreak of Corona Virus Disease 2019 in China in early 2020, Chinese people have been quarantined at home many times and outdoor activities have been restricted. The prevalence rate of myopia among school-age children has increased[29], and young children are in a critical period of vision development, and more sensitive to environmental changes, so myopia deviation is more obvious[30]. The increasing prevalence of myopia during early childhood has heightened the risk of developing high myopia in adulthood, and the pathological consequences include posterior scleral staphyloma, choroidal retinal atrophy, macular degeneration, and other related eye disease, which are the main causes of visual impairment and blindness[31-32]. Scholars have never stopped the study of myopia, but the specific molecular mechanism of myopia is still unclear.

Molecular Mechanism of Hypoxia Reducing Collagen Expression in Scleral Fibroblasts Studies have shown that collagen levels in human scleral fibroblasts are reduced after ambient oxygen concentration is reduced to 5%[10]. In contrast, in triple-negative breast cancer cells, hypoxia activates lysyl oxidase, which leads to the cross-linking and stabilization of extracellular matrix proteins, especially collagen type I, by

mediating the conversion of lysine residues in collagen and elastin precursors to highly active aldehydes[33]. Therefore, the expression of collagen is affected by many factors. In different cells or different physiological and pathological states, hypoxia treatment may have opposite effects on collagen content.

The main protein in the sclera is collagen. Among HYP *vs* Control differentially expressed genes, *HIF-1* is considered to be the main coordinator of cellular adaptive response to hypoxia, which can affect a variety of indicators including the extracellular matrix. *ANGPT4* is the target product of *HIF-1* transcription[34], while *NDUFA4L2* is a target of *HIF*, and its induction by *HIF-1* is related to the decrease of mitochondrial oxygen consumption, thus reducing the production of reactive oxygen[35]. MMP-2 increased in myopia, and collagen type I synthesis decreased significantly, resulting in an imbalance, the lower the ratio of collagen type I to collagen type V, the smaller the diameter of collagen fibril[36-37] and promote myopia. Hypoxia-sensitive gene *Ca9* decreases and promotes basement membrane assembly (collagen type IV α1) at high oxygen levels[38], whereas hypoxia expression increases. Other studies have shown that the expression of *LRRC15* in fibroblasts inhibits collagen production[39]. In *ISG15* deficient cells, collagen and adhesion molecules decreased and MMP increased[40-41].

Hypoxia deactivates Hippo signaling[42], *MOB1B* is a core component of the Hippo signaling pathway and is crucial for the expression of collagen type XVII protein[43]. In zebrafish, the potential loss of *LRRC4C* leads to myopia displacement in axial elongation and refractive state[44].

GO and KEGG analysis showed that the above-related differentially expressed genes were enriched in carbon-oxygen lyase activity, ion channel correlation and other molecular functions and cell components, biological processes of glycolysis, the HIF-1, and the PPAR signaling pathways. extracellular *ENO1* in the crosstalk with the intracellular glycolytic pathway *via* HIF-1α[45]. Because ion channels exist widely in the body and participate in basic biological processes, the study of channel-related lesions has always aroused great interest in scientific and medical circles[46]. In addition, transepithelial transport of ions and/or fluids in the retinal pigment epithelium can affect the growth of the eyes[47]. In a form-deprivation myopia-induced guinea pig model, glycolysis is associated with atropine treatment of myopia[48]. Hypoxia also activates the HIF-1α signaling pathway and reduces collagen expression[10]. Activation of the PPAR-γ signaling pathway can reduce collagen synthesis and partially inhibit airway fibrosis in the treatment of asthma[49], and when the expression or activity of PPAR-γ is inhibited, its effect on reducing α-smooth muscle actin and collagen type I expression is inhibited[50].

In conclusion, hypoxia-induced changes in gene expression, particularly those related to collagen regulation, contribute significantly to the understanding of myopia's molecular underpinnings. The interplay between hypoxia, HIF-1 signaling, and extracellular matrix components provides a comprehensive perspective on the complex mechanisms driving myopia development.

Molecular Mechanism of α-KG Enhancing Collagen Expression in Scleral Fibroblasts under Hypoxia In recent years, most of the research on myopia at home and abroad is on the sclera. By inducing experimental myopia in guinea pigs, the biomechanical changes of myopic sclera were studied by frozen sections[51]. MMP-2 is proven to participate in the scleral development of form-deprivation myopia in guinea pigs[52]. Scleral cross-linking is a potential treatment for controlling myopia progression[53], and other treatment options such as slowing myopia progression through scleral fibroblast transplantation[54] have great limitations. However, nightly use of 0.05% atropine eyedrops compared with placebo resulted in a significantly lower incidence of myopia and a lower percentage of participants with fast myopic shift at 2y, further research is needed to replicate the findings[55]. The 7-methylxanthine can increase collagen concentration and collagen fibrils diameter in the posterior sclera[56]. Clinical trials on myopic children have shown that 7-methylxanthine can reduce axial elongation of the eye and myopia progression[57], but the specific mechanism is still unknown. The metabolic molecule α-KG is closely related to hypoxia, the HIF-1α signaling pathway, and collagen synthesis has become the focus of follow-up research. α-KG is an intermediate metabolite of the human biochemical process, which is relatively safe. It can be used as a substrate molecule to participate in biochemical reactions regulated by the HIF-1α signaling pathway, regulate the occurrence and development of diseases by inhibiting the HIF-1α signaling pathway, and also participate in the biosynthesis process of proline hydroxylation modification of collagen peptide chain in cells. Whether α-KG can regulate scleral remodeling and myopia development has not been reported in the literature. Ge *et al*[15] found that α-KG promotes collagen translation and stability by mediating mammalian target of rapamycin (mTOR) activation and proline hydroxylation. The conclusion of this experiment, α-KG increases the production and stability of collagen, and when the expression of collagen is reduced in hypoxia treatment, the addition of α-KG can restore the content of collagen. HIF-1α proline hydroxylation is an indispensable step in the HIF-1α ubiquitination degradation process. In the presence of oxygen, α-KG and oxygen participate in the reaction to hydroxylate the proline on HIF-1α, thus entering the HIF-1α ubiquitination process.

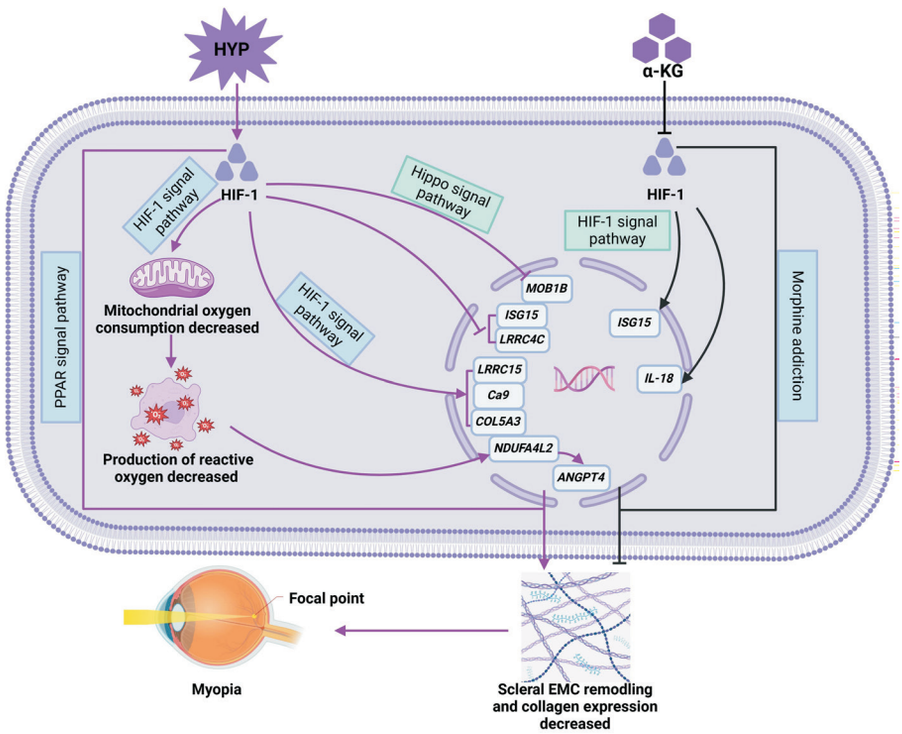

Figure 12 Possible mechanisms of hypoxia and α-KG influencing myopia KG: Ketoglutaric acid.

In addition, in the differentially expressed genes and enrichment pathways of HYP+α-KG *vs* HYP, the change of *ISG15* expression is contrary to that of hypoxia, and the addition of α-KG increases the expression of *ISG15*, thereby increasing the expression of collagen[40-41]. In the absence of interleukin-18 (IL-18) signaling, collagen deposition, and key fibrosis-related genes are reduced[58].

GO and KEGG analysis showed that these differential genes were mainly concentrated in cytoskeleton-related molecular functions, cell components, biological processes, and the Morphine addiction pathway. Studies have shown that keratinocyte migration and cytoskeletal structural components are weakened in high myopia[59]. Simian immunodeficiency virus-infected rhesus macaques exposed to morphine increased accumulation of interstitial collagen[60].

In summary, α-KG's ability to counteract hypoxia-induced changes in gene expression, particularly in relation to collagen, positions it as a promising candidate for myopia control. Further investigations into the specific mechanisms and potential applications of α-KG in myopia treatment are essential for advancing our understanding and developing effective interventions.

In this study, the transcriptome of rabbit scleral fibroblasts treated with HYP and HYP+α-KG was compared and analyzed to explore the genes and related pathways of hypoxia and α-KG influencing myopia, as shown in Figure 12, we identified genes and other metabolic pathways with collagen metabolism and hypoxia signaling pathways related to myopia and identified new genes related to hypoxia and α-KG by RT-qPCR, which may contribute to the prevention and control of myopia. By comparing the gene expression patterns of different treatments, the molecular mechanism of myopia occurrence and development will be further revealed.

ACKNOWLEDGEMENTS

Foundations: Supported by the Natural Science Foundation of Shandong Province, China (No.ZR2023MA069); the Medical and Health Technology Development Project of Shandong Province, China (No.202202050602); College Students' Innovation and Entrepreneurship Training Program (No. S202410438017); the Graduate Student Research Grant from Shandong Second Medical University.

Conflicts of Interest: Sun Y, None; **Li ZZ**, None; **Yang J,** None; **Sha YR**, None; **Hou XY,** None; **Fu H,** None; **Li JY,** None; **Bai SC,** None; **Xie YF,** None; **Wang GH,** None.

REFERENCES

1 Baird PN, Saw SM, Lanca C, *et al*. Myopia. *Nat Rev Dis Primers* 2020;6(1):99.

2 Zadnik K, Schulman E, Flitcroft I, *et al*, Trial Group Investigators CHAMP. Efficacy and safety of 0.01% and 0.02% atropine for the treatment of pediatric myopia progression over 3 years: a randomized clinical trial. *JAMA Ophthalmol* 2023;141(10):990-999.

3 Umaefulam V, Safi S, Lingham G, *et al*. Approaches for delivery of refractive and optical care services in community and primary care settings. *Cochrane Database Syst Rev* 2024;5(5):CD016043.

4 Du R, Xie SQ, Igarashi-Yokoi T, Watanabe T, Uramoto K, Takahashi H, Nakao N, Yoshida T, Fang YX, Ohno-Matsui K. Continued increase of axial length and its risk factors in adults with high myopia. *JAMA Ophthalmol* 2021;139(10):1096-1103.

5 Boote C, Sigal IA, Grytz R, Hua Y, Nguyen TD, Girard MJA. Scleral structure and biomechanics. *Prog Retin Eye Res* 2020;74:100773.

6 McBrien NA, Gentle A. Role of the sclera in the development and pathological complications of myopia. *Prog Retin Eye Res* 2003;22(3):307-338.

7 Xie YF, Ouyang XL, Wang GH. Mechanical strain affects collagen metabolism-related gene expression in scleral fibroblasts. *Biomed Pharmacother* 2020;126:110095.

8 Wu H, Zhang GY, Shen MX, *et al*. Assessment of choroidal vascularity and choriocapillaris blood perfusion in anisomyopic adults by SS-OCT/OCTA. *Invest Ophthalmol Vis Sci* 2021;62(1):8.

9 Chang XJ, Li M, Lv L, Yan XQ, Liu Y, Zhu MX, Wang JM, Wang P, Xiang Y. Assessment of choroidal vascularity and choriocapillaris blood perfusion after accommodation in myopia, emmetropia, and hyperopia groups among children. *Front Physiol* 2022;13:854240.

10 Wu H, Chen W, Zhao F, *et al*. Scleral hypoxia is a target for myopia control. *Proc Natl Acad Sci U S A* 2018;115(30):E7091-E7100.

11 Wu WJ, Su YC, Hu CX, Tao HX, Jiang Y, Zhu GD, Zhu JD, Zhai Y, Qu J, Zhou XT, Zhao F. Hypoxia-induced scleral HIF-2α upregulation contributes to rises in MMP-2 expression and myopia development in mice. *Invest Ophthalmol Vis Sci* 2022;63(8):2.

12 Gilkes DM, Bajpai S, Chaturvedi P, Wirtz D, Semenza GL. Hypoxia-inducible factor 1 (HIF-1) promotes extracellular matrix remodeling under hypoxic conditions by inducing P4HA1, P4HA2, and PLOD2 expression in fibroblasts. *J Biol Chem* 2013;288(15):10819-10829.

13 Wang QF, Wang P, Qin ZL, Yang X, Pan BL, Nie FF, Bi HS. Altered glucose metabolism and cell function in keloid fibroblasts under hypoxia. *Redox Biol* 2021;38:101815.

14 Elia I, Rossi M, Stegen S, *et al*. Breast cancer cells rely on environmental pyruvate to shape the metastatic niche. *Nature* 2019;568(7750):117-121.

15 Ge J, Cui HC, Xie N, Banerjee S, Guo SJ, Dubey S, Barnes S, Liu G. Glutaminolysis promotes collagen translation and stability via α-ketoglutarate-mediated mTOR activation and proline hydroxylation. *Am J Respir Cell Mol Biol* 2018;58(3):378-390.

16 Xiong GF, Stewart RL, Chen J, Gao TY, Scott TL, Samayoa LM, O'Connor K, Lane AN, Xu R. Collagen prolyl 4-hydroxylase 1 is essential for HIF-1α stabilization and TNBC chemoresistance. *Nat Commun* 2018;9(1):4456.

17 Xu QH, Norman JT, Shrivastav S, Lucio-Cazana J, Kopp JB. *In vitro* models of TGF-beta-induced fibrosis suitable for high-throughput screening of antifibrotic agents. *Am J Physiol Renal Physiol* 2007;293(2):F631-F640.

18 El-Shazly AA, Farweez YA, ElSebaay ME, El-Zawahry WMA. Correlation between choroidal thickness and degree of myopia assessed with enhanced depth imaging optical coherence tomography. *Eur J Ophthalmol* 2017;27(5):577-584.

19 Min CH, Al-Qattan HM, Lee JY, Kim JG, Yoon YH, Kim YJ. Macular microvasculature in high myopia without pathologic changes: an optical coherence tomography angiography study. *Korean J Ophthalmol* 2020;34(2):106-112.

20 Duan F, Yuan ZH, Deng JY, Wong YL, Yeo AC, Chen X. Choroidal thickness and associated factors among adult myopia: a baseline report from a medical university student cohort. *Ophthalmic Epidemiol* 2019;26(4):244-250.

21 Xie JM, Ye LY, Chen QY, Shi Y, Hu GY, Yin Y, Zou HD, Zhu JF, Fan Y, He JN, Xu X. Choroidal thickness and its association with age, axial length, and refractive error in Chinese adults. *Invest Ophthalmol Vis Sci* 2022;63(2):34.

22 Teberik K, Kaya M. Retinal and choroidal thickness in patients with high myopia without maculopathy. *Pak J Med Sci* 2017;33(6):1438-1443.

23 Al-Sheikh M, Phasukkijwatana N, Dolz-Marco R, Rahimi M, Iafe NA, Freund KB, Sadda SR, Sarraf D. Quantitative OCT angiography of the retinal microvasculature and the choriocapillaris in myopic eyes. *Invest Ophthalmol Vis Sci* 2017;58(4):2063-2069.

24 Sung MS, Lee TH, Heo H, Park SW. Association between optic nerve head deformation and retinal microvasculature in high myopia. *Am J Ophthalmol* 2018;188:81-90.

25 Gupta P, Thakku SG, Saw SM, Tan M, Lim E, Tan M, Cheung CMG, Wong TY, Cheng CY. Characterization of choroidal morphologic and vascular features in young men with high myopia using spectral-domain optical coherence tomography. *Am J Ophthalmol* 2017;177:27-33.

26 Yang SQ, Zhou MW, Lu B, Zhang PF, Zhao JK, Kang M, Wang RS, Wang FH, Sun XD. Quantification of macular vascular density using optical coherence tomography angiography and its relationship with retinal thickness in myopic eyes of young adults. *J Ophthalmol* 2017;2017:1397179.

27 Guo Y, Sung MS, Park SW. Assessment of superficial retinal microvascular density in healthy myopia. *Int Ophthalmol* 2019;39(8):1861-1870.

28 Alzaben Z, Cardona G, Zapata MA, Zaben A. Interocular asymmetry in choroidal thickness and retinal sensitivity in high myopia. *Retina* 2018;38(8):1620-1628.

29 Hu Y, Zhao F, Ding XH, *et al*. Rates of myopia development in young Chinese schoolchildren during the outbreak of COVID-19. *JAMA Ophthalmol* 2021;139(10):1115-1121.

30 Wang JX, Li Y, Musch DC, *et al*. Progression of myopia in school-aged children after COVID-19 home confinement. *JAMA Ophthalmol* 2021;139(3):293-300.

31 Biswas S, El Kareh A, Qureshi M, Lee DMX, Sun CH, Lam JSH, Saw SM, Najjar RP. The influence of the environment and lifestyle on myopia. *J Physiol Anthropol* 2024;43(1):7.

32 Ohno-Matsui K, Lai TYY, Lai CC, Cheung CMG. Updates of pathologic myopia. *Prog Retin Eye Res* 2016;52:156-187.

33 Saatci O, Kaymak A, Raza U, *et al*. Targeting lysyl oxidase (LOX) overcomes chemotherapy resistance in triple negative breast cancer. *Nat Commun* 2020;11(1):2416.

34 Andrikopoulou E, Zhang X, Sebastian R, Marti G, Liu L, Milner SM, Harmon JW. Current insights into the role of HIF-1 in cutaneous wound healing. *Curr Mol Med* 2011;11(3):218-235.

35 Piltti J, Bygdell J, Qu CJ, Lammi MJ. Effects of long-term low oxygen tension in human chondrosarcoma cells. *J Cell Biochem* 2018;119(2):2320-2332.

36 Siegwart JT Jr, Norton TT. Steady state mRNA levels in tree shrew sclera with form-deprivation myopia and during recovery. *Invest Ophthalmol Vis Sci* 2001;42(6):1153-1159.

37 Stanton CM, Findlay AS, Drake C, Mustafa MZ, Gautier P, McKie L, Jackson IJ, Vitart V. A mouse model of brittle cornea syndrome caused by mutation in Zfp469. *Dis Model Mech* 2021;14(9):dmm049175.

38 Aplin AC, Nicosia RF. Tissue oxygenation stabilizes neovessels and mitigates hemorrhages in human atherosclerosis-induced angiogenesis. *Angiogenesis* 2023;26(1):63-76.

39 Loo L, Waller MA, Moreno CL, *et al.* Fibroblast-expressed LRRC15 is a receptor for SARS-CoV-2 spike and controls antiviral and antifibrotic transcriptional programs. *PLoS Biol* 2023;21(2):e3001967.

40 Yeh YH, Yang YC, Hsieh MY, Yeh YC, Li TK. A negative feedback of the HIF-1α pathway via interferon-stimulated gene 15 and ISGylation. *Clin Cancer Res* 2013;19(21):5927-5939.

41 Malik MNH, Waqas SFUH, Zeitvogel J, *et al*. Congenital deficiency reveals critical role of ISG15 in skin homeostasis. *J Clin Invest* 2022;132(3):e141573.

42 Ma B, Chen Y, Chen L, *et al*. Hypoxia regulates Hippo signalling through the SIAH2 ubiquitin E3 ligase. *Nat Cell Biol* 2015;17(1):95-103.

43 Otsubo K, Goto H, Nishio M, *et al*. MOB1-YAP1/TAZ-NKX2.1 axis controls bronchioalveolar cell differentiation, adhesion and tumour formation. *Oncogene* 2017;36(29):4201-4211.

44 Quint WH, Tadema KCD, Kokke NCCJ, Meester-Smoor MA, Miller AC, Willemsen R, Klaver CCW, Iglesias AI. Post-GWAS screening of candidate genes for refractive error in mutant zebrafish models. *Sci Rep* 2023;13(1):2017.

45 Chung IC, Huang WC, Huang YT, Chen ML, Tsai AW, Wu PY, Yuan TT. Unrevealed roles of extracellular enolase-1 (ENO1) in promoting glycolysis and pro-cancer activities in multiple myeloma via hypoxia-inducible factor 1α. *Oncol Rep* 2023;50(5):205.

46 Rashwan R, Hunt DM, Carvalho LS. The role of voltage-gated ion channels in visual function and disease in mammalian photoreceptors. *Pflügers Arch Eur J Physiol* 2021;473(9):1455-1468.

47 Zhang Y, Wildsoet CF. RPE and choroid mechanisms underlying ocular growth and myopia. *Prog Mol Biol Transl Sci* 2015;134:221-240.

48 Zhu Y, Bian JF, Lu DQ, To CH, Lam CSY, Li KK, Yu FJ, Gong BT, Wang Q, Ji XW, Zhang HM, Nian H, Lam TC, Wei RH. Alteration of EIF2 signaling, glycolysis, and dopamine secretion in form-deprived myopia in response to 1% atropine treatment: evidence from interactive iTRAQ-MS and SWATH-MS proteomics using a guinea pig model. *Front Pharmacol* 2022;13:814814.

49 Lu JM, Liu L, Zhu YT, *et al*. PPAR-γ inhibits IL-13-induced collagen production in mouse airway fibroblasts. *Eur J Pharmacol* 2014;737:133-139.

50 Hua QZ, Huang XT, Xie WX, *et al*. PPARγ mediates the anti-pulmonary fibrosis effect of icaritin. *Toxicol Lett* 2021;350:81-90.

51 Hoerig C, McFadden S, Hoang QV, Mamou J. Biomechanical changes in myopic sclera correlate with underlying changes in microstructure. *Exp Eye Res* 2022;224:109165.

52 Liu YX, Sun Y. MMP-2 participates in the sclera of guinea pig with form-deprivation myopia via IGF-1/STAT3 pathway. *Eur Rev Med Pharmacol Sci* 2018;22(9):2541-2548.

53 Sankaridurg P, Berntsen DA, Bullimore MA, *et al*. IMI 2023 digest. *Invest Ophthalmol Vis Sci* 2023;64(6):7.

54 Shinohara K, Yoshida T, Liu HD, Ichinose S, Ishida T, Nakahama KI, Nagaoka N, Moriyama M, Morita I, Ohno-Matsui K. Establishment of novel therapy to reduce progression of myopia in rats with experimental myopia by fibroblast transplantation on sclera. *J Tissue Eng Regen Med* 2018;12(1):e451-e461.

55 Yam JC, Zhang XJ, Zhang YZ, *et al*. Effect of low-concentration atropine eyedrops vs placebo on myopia incidence in children: the LAMP2 randomized clinical trial. *JAMA* 2023;329(6):472-481.

56 Trier K, Olsen EB, Kobayashi T, Ribel-Madsen SM. Biochemical and ultrastructural changes in rabbit sclera after treatment with 7-methylxanthine, theobromine, acetazolamide, or L-ornithine. *Br J Ophthalmol* 1999;83(12):1370-1375.

57 Trier K, Munk Ribel-Madsen S, Cui DM, Brøgger Christensen S. Systemic 7-methylxanthine in retarding axial eye growth and myopia progression: a 36-month pilot study. *J Ocul Biol Dis Infor* 2008;1(2-4):85-93.

58 Knorr J, Kaufmann B, Inzaugarat ME, *et al*. Interleukin-18 signaling promotes activation of hepatic stellate cells in mouse liver fibrosis. *Hepatology* 2023;77(6):1968-1982.

59 Wu WJ, Xu YS, Zhang FJ. Comparisons of the protein expressions between high myopia and moderate myopia on the anterior corneal stroma in human. *Graefes Arch Clin Exp Ophthalmol* 2023;261(12):3549-3558.

60 Chemparathy DT, Sil S, Callen S, *et al*. Inflammation-associated lung tissue remodeling and fibrosis in morphine-dependent SIV-infected macaques. *Am J Pathol* 2023;193(4):380-391.